BABAR-PUB-07/067
SLAC-PUB-13021
arXiv:0711.4889 [hep-ex]

Measurement of the $B \to X_s\gamma$ Branching Fraction and Photon Energy Spectrum using the Recoil Method

B. Aubert,[1] M. Bona,[1] Y. Karyotakis,[1] J. P. Lees,[1] V. Poireau,[1] X. Prudent,[1] V. Tisserand,[1] A. Zghiche,[1] J. Garra Tico,[2] E. Grauges,[2] L. Lopez,[3] A. Palano,[3] M. Pappagallo,[3] G. Eigen,[4] B. Stugu,[4] L. Sun,[4] G. S. Abrams,[5] M. Battaglia,[5] D. N. Brown,[5] J. Button-Shafer,[5] R. N. Cahn,[5] R. G. Jacobsen,[5] J. A. Kadyk,[5] L. T. Kerth,[5] Yu. G. Kolomensky,[5] G. Kukartsev,[5] D. Lopes Pegna,[5] G. Lynch,[5] T. J. Orimoto,[5] I. L. Osipenkov,[5] M. T. Ronan,[5,*] K. Tackmann,[5] T. Tanabe,[5] W. A. Wenzel,[5] P. del Amo Sanchez,[6] C. M. Hawkes,[6] N. Soni,[6] A. T. Watson,[6] H. Koch,[7] T. Schroeder,[7] D. Walker,[8] D. J. Asgeirsson,[9] T. Cuhadar-Donszelmann,[9] B. G. Fulsom,[9] C. Hearty,[9] T. S. Mattison,[9] J. A. McKenna,[9] M. Barrett,[10] A. Khan,[10] M. Saleem,[10] L. Teodorescu,[10] V. E. Blinov,[11] A. D. Bukin,[11] A. R. Buzykaev,[11] V. P. Druzhinin,[11] V. B. Golubev,[11] A. P. Onuchin,[11] S. I. Serednyakov,[11] Yu. I. Skovpen,[11] E. P. Solodov,[11] K. Yu. Todyshev,[11] M. Bondioli,[12] S. Curry,[12] I. Eschrich,[12] D. Kirkby,[12] A. J. Lankford,[12] P. Lund,[12] M. Mandelkern,[12] E. C. Martin,[12] D. P. Stoker,[12] S. Abachi,[13] C. Buchanan,[13] J. W. Gary,[14] F. Liu,[14] O. Long,[14] B. C. Shen,[14,*] G. M. Vitug,[14] L. Zhang,[14] H. P. Paar,[15] S. Rahatlou,[15] V. Sharma,[15] J. W. Berryhill,[16] C. Campagnari,[16] A. Cunha,[16] B. Dahmes,[16] T. M. Hong,[16] D. Kovalskyi,[16] J. D. Richman,[16] T. W. Beck,[17] A. M. Eisner,[17] C. J. Flacco,[17] C. A. Heusch,[17] J. Kroseberg,[17] W. S. Lockman,[17] T. Schalk,[17] B. A. Schumm,[17] A. Seiden,[17] M. G. Wilson,[17] L. O. Winstrom,[17] E. Chen,[18] C. H. Cheng,[18] B. Echenard,[18] F. Fang,[18] D. G. Hitlin,[18] I. Narsky,[18] T. Piatenko,[18] F. C. Porter,[18] R. Andreassen,[19] G. Mancinelli,[19] B. T. Meadows,[19] K. Mishra,[19] M. D. Sokoloff,[19] F. Blanc,[20] P. C. Bloom,[20] W. T. Ford,[20] J. F. Hirschauer,[20] A. Kreisel,[20] M. Nagel,[20] U. Nauenberg,[20] A. Olivas,[20] J. G. Smith,[20] K. A. Ulmer,[20] S. R. Wagner,[20] J. Zhang,[20] R. Ayad,[21,†] A. M. Gabareen,[21] A. Soffer,[21,‡] W. H. Toki,[21] R. J. Wilson,[21] D. D. Altenburg,[22] E. Feltresi,[22] A. Hauke,[22] H. Jasper,[22] J. Merkel,[22] A. Petzold,[22] B. Spaan,[22] K. Wacker,[22] V. Klose,[23] M. J. Kobel,[23] H. M. Lacker,[23] W. F. Mader,[23] R. Nogowski,[23] J. Schubert,[23] K. R. Schubert,[23] R. Schwierz,[23] J. E. Sundermann,[23] A. Volk,[23] D. Bernard,[24] G. R. Bonneaud,[24] E. Latour,[24] V. Lombardo,[24] Ch. Thiebaux,[24] M. Verderi,[24] P. J. Clark,[25] W. Gradl,[25] F. Muheim,[25] S. Playfer,[25] A. I. Robertson,[25] J. E. Watson,[25] Y. Xie,[25] M. Andreotti,[26] D. Bettoni,[26] C. Bozzi,[26] R. Calabrese,[26] A. Cecchi,[26] G. Cibinetto,[26] P. Franchini,[26] E. Luppi,[26] M. Negrini,[26] A. Petrella,[26] L. Piemontese,[26] E. Prencipe,[26] V. Santoro,[26] F. Anulli,[27] R. Baldini-Ferroli,[27] A. Calcaterra,[27] R. de Sangro,[27] G. Finocchiaro,[27] S. Pacetti,[27] P. Patteri,[27] I. M. Peruzzi,[27,§] M. Piccolo,[27] M. Rama,[27] A. Zallo,[27] A. Buzzo,[28] R. Contri,[28] M. Lo Vetere,[28] M. M. Macri,[28] M. R. Monge,[28] S. Passaggio,[28] C. Patrignani,[28] E. Robutti,[28] A. Santroni,[28] S. Tosi,[28] K. S. Chaisanguanthum,[29] M. Morii,[29] J. Wu,[29] R. S. Dubitzky,[30] J. Marks,[30] S. Schenk,[30] U. Uwer,[30] D. J. Bard,[31] P. D. Dauncey,[31] J. A. Nash,[31] W. Panduro Vazquez,[31] M. Tibbetts,[31] P. K. Behera,[32] X. Chai,[32] M. J. Charles,[32] U. Mallik,[32] J. Cochran,[33] H. B. Crawley,[33] L. Dong,[33] V. Eyges,[33] W. T. Meyer,[33] S. Prell,[33] E. I. Rosenberg,[33] A. E. Rubin,[33] Y. Y. Gao,[34] A. V. Gritsan,[34] Z. J. Guo,[34] C. K. Lae,[34] A. G. Denig,[35] M. Fritsch,[35] G. Schott,[35] N. Arnaud,[36] J. Béquilleux,[36] A. D'Orazio,[36] M. Davier,[36] G. Grosdidier,[36] A. Höcker,[36] V. Lepeltier,[36] F. Le Diberder,[36] A. M. Lutz,[36] S. Pruvot,[36] P. Roudeau,[36] M. H. Schune,[36] J. Serrano,[36] V. Sordini,[36] A. Stocchi,[36] W. F. Wang,[36] G. Wormser,[36] D. J. Lange,[37] D. M. Wright,[37] I. Bingham,[38] J. P. Burke,[38] C. A. Chavez,[38] J. R. Fry,[38] E. Gabathuler,[38] R. Gamet,[38] D. E. Hutchcroft,[38] D. J. Payne,[38] K. C. Schofield,[38] C. Touramanis,[38] A. J. Bevan,[39] K. A. George,[39] F. Di Lodovico,[39] R. Sacco,[39] G. Cowan,[40] H. U. Flaecher,[40] D. A. Hopkins,[40] S. Paramesvaran,[40] F. Salvatore,[40] A. C. Wren,[40] D. N. Brown,[41] C. L. Davis,[41] N. R. Barlow,[42] R. J. Barlow,[42] Y. M. Chia,[42] C. L. Edgar,[42] G. D. Lafferty,[42] T. J. West,[42] J. I. Yi,[42] J. Anderson,[43] C. Chen,[43] A. Jawahery,[43] D. A. Roberts,[43] G. Simi,[43] J. M. Tuggle,[43] C. Dallapiccola,[44] S. S. Hertzbach,[44] X. Li,[44] T. B. Moore,[44] E. Salvati,[44] S. Saremi,[44] R. Cowan,[45] D. Dujmic,[45] P. H. Fisher,[45] K. Koeneke,[45] G. Sciolla,[45] M. Spitznagel,[45] F. Taylor,[45] R. K. Yamamoto,[45] M. Zhao,[45] S. E. Mclachlin,[46,*] P. M. Patel,[46] S. H. Robertson,[46] A. Lazzaro,[47] F. Palombo,[47] J. M. Bauer,[48] L. Cremaldi,[48] V. Eschenburg,[48] R. Godang,[48] R. Kroeger,[48] D. A. Sanders,[48] D. J. Summers,[48] H. W. Zhao,[48] S. Brunet,[49] D. Côté,[49] M. Simard,[49] P. Taras,[49] F. B. Viaud,[49] H. Nicholson,[50] G. De Nardo,[51] F. Fabozzi,[51,¶] L. Lista,[51] D. Monorchio,[51] C. Sciacca,[51] M. A. Baak,[52] G. Raven,[52]

H. L. Snoek,[52] C. P. Jessop,[53] K. J. Knoepfel,[53] J. M. LoSecco,[53] G. Benelli,[54] L. A. Corwin,[54] K. Honscheid,[54] H. Kagan,[54] R. Kass,[54] J. P. Morris,[54] A. M. Rahimi,[54] J. J. Regensburger,[54] S. J. Sekula,[54] Q. K. Wong,[54] N. L. Blount,[55] J. Brau,[55] R. Frey,[55] O. Igonkina,[55] J. A. Kolb,[55] M. Lu,[55] R. Rahmat,[55] N. B. Sinev,[55] D. Strom,[55] J. Strube,[55] E. Torrence,[55] N. Gagliardi,[56] A. Gaz,[56] M. Margoni,[56] M. Morandin,[56] A. Pompili,[56] M. Posocco,[56] M. Rotondo,[56] F. Simonetto,[56] R. Stroili,[56] C. Voci,[56] E. Ben-Haim,[57] H. Briand,[57] G. Calderini,[57] J. Chauveau,[57] P. David,[57] L. Del Buono,[57] Ch. de la Vaissière,[57] O. Hamon,[57] Ph. Leruste,[57] J. Malclès,[57] J. Ocariz,[57] A. Perez,[57] J. Prendki,[57] L. Gladney,[58] M. Biasini,[59] R. Covarelli,[59] E. Manoni,[59] C. Angelini,[60] G. Batignani,[60] S. Bettarini,[60] M. Carpinelli,[60, **] R. Cenci,[60] A. Cervelli,[60] F. Forti,[60] M. A. Giorgi,[60] A. Lusiani,[60] G. Marchiori,[60] M. A. Mazur,[60] M. Morganti,[60] N. Neri,[60] E. Paoloni,[60] G. Rizzo,[60] J. J. Walsh,[60] J. Biesiada,[61] Y. P. Lau,[61] C. Lu,[61] J. Olsen,[61] A. J. S. Smith,[61] A. V. Telnov,[61] E. Baracchini,[62] F. Bellini,[62] G. Cavoto,[62] D. del Re,[62] E. Di Marco,[62] R. Faccini,[62] F. Ferrarotto,[62] F. Ferroni,[62] M. Gaspero,[62] P. D. Jackson,[62] M. A. Mazzoni,[62] S. Morganti,[62] G. Piredda,[62] F. Polci,[62] F. Renga,[62] C. Voena,[62] M. Ebert,[63] T. Hartmann,[63] H. Schröder,[63] R. Waldi,[63] T. Adye,[64] G. Castelli,[64] B. Franek,[64] E. O. Olaiya,[64] W. Roethel,[64] F. F. Wilson,[64] S. Emery,[65] M. Escalier,[65] A. Gaidot,[65] S. F. Ganzhur,[65] G. Hamel de Monchenault,[65] W. Kozanecki,[65] G. Vasseur,[65] Ch. Yèche,[65] M. Zito,[65] X. R. Chen,[66] H. Liu,[66] W. Park,[66] M. V. Purohit,[66] R. M. White,[66] J. R. Wilson,[66] M. T. Allen,[67] D. Aston,[67] R. Bartoldus,[67] P. Bechtle,[67] R. Claus,[67] J. P. Coleman,[67] M. R. Convery,[67] J. C. Dingfelder,[67] J. Dorfan,[67] G. P. Dubois-Felsmann,[67] W. Dunwoodie,[67] R. C. Field,[67] T. Glanzman,[67] S. J. Gowdy,[67] M. T. Graham,[67] P. Grenier,[67] C. Hast,[67] W. R. Innes,[67] J. Kaminski,[67] M. H. Kelsey,[67] H. Kim,[67] P. Kim,[67] M. L. Kocian,[67] D. W. G. S. Leith,[67] S. Li,[67] S. Luitz,[67] V. Luth,[67] H. L. Lynch,[67] D. B. MacFarlane,[67] H. Marsiske,[67] R. Messner,[67] D. R. Muller,[67] S. Nelson,[67] C. P. O'Grady,[67] I. Ofte,[67] A. Perazzo,[67] M. Perl,[67] T. Pulliam,[67] B. N. Ratcliff,[67] A. Roodman,[67] A. A. Salnikov,[67] R. H. Schindler,[67] J. Schwiening,[67] A. Snyder,[67] D. Su,[67] M. K. Sullivan,[67] K. Suzuki,[67] S. K. Swain,[67] J. M. Thompson,[67] J. Va'vra,[67] A. P. Wagner,[67] M. Weaver,[67] W. J. Wisniewski,[67] M. Wittgen,[67] D. H. Wright,[67] H. W. Wulsin,[67] A. K. Yarritu,[67] K. Yi,[67] C. C. Young,[67] V. Ziegler,[67] P. R. Burchat,[68] A. J. Edwards,[68] S. A. Majewski,[68] T. S. Miyashita,[68] B. A. Petersen,[68] L. Wilden,[68] S. Ahmed,[69] M. S. Alam,[69] R. Bula,[69] J. A. Ernst,[69] B. Pan,[69] M. A. Saeed,[69] S. B. Zain,[69] S. M. Spanier,[70] B. J. Wogsland,[70] R. Eckmann,[71] J. L. Ritchie,[71] A. M. Ruland,[71] C. J. Schilling,[71] R. F. Schwitters,[71] J. M. Izen,[72] X. C. Lou,[72] S. Ye,[72] F. Bianchi,[73] F. Gallo,[73] D. Gamba,[73] M. Pelliccioni,[73] M. Bomben,[74] L. Bosisio,[74] C. Cartaro,[74] F. Cossutti,[74] G. Della Ricca,[74] L. Lanceri,[74] L. Vitale,[74] V. Azzolini,[75] N. Lopez-March,[75] F. Martinez-Vidal,[75] D. A. Milanes,[75] A. Oyanguren,[75] J. Albert,[76] Sw. Banerjee,[76] B. Bhuyan,[76] K. Hamano,[76] R. Kowalewski,[76] I. M. Nugent,[76] J. M. Roney,[76] R. J. Sobie,[76] P. F. Harrison,[77] J. Ilic,[77] T. E. Latham,[77] G. B. Mohanty,[77] H. R. Band,[78] X. Chen,[78] S. Dasu,[78] K. T. Flood,[78] J. J. Hollar,[78] P. E. Kutter,[78] Y. Pan,[78] M. Pierini,[78] R. Prepost,[78] S. L. Wu,[78] and H. Neal[79]

(The *BABAR* Collaboration)

[1] *Laboratoire de Physique des Particules, IN2P3/CNRS et Université de Savoie, F-74941 Annecy-Le-Vieux, France*
[2] *Universitat de Barcelona, Facultat de Fisica, Departament ECM, E-08028 Barcelona, Spain*
[3] *Università di Bari, Dipartimento di Fisica and INFN, I-70126 Bari, Italy*
[4] *University of Bergen, Institute of Physics, N-5007 Bergen, Norway*
[5] *Lawrence Berkeley National Laboratory and University of California, Berkeley, California 94720, USA*
[6] *University of Birmingham, Birmingham, B15 2TT, United Kingdom*
[7] *Ruhr Universität Bochum, Institut für Experimentalphysik 1, D-44780 Bochum, Germany*
[8] *University of Bristol, Bristol BS8 1TL, United Kingdom*
[9] *University of British Columbia, Vancouver, British Columbia, Canada V6T 1Z1*
[10] *Brunel University, Uxbridge, Middlesex UB8 3PH, United Kingdom*
[11] *Budker Institute of Nuclear Physics, Novosibirsk 630090, Russia*
[12] *University of California at Irvine, Irvine, California 92697, USA*
[13] *University of California at Los Angeles, Los Angeles, California 90024, USA*
[14] *University of California at Riverside, Riverside, California 92521, USA*
[15] *University of California at San Diego, La Jolla, California 92093, USA*
[16] *University of California at Santa Barbara, Santa Barbara, California 93106, USA*
[17] *University of California at Santa Cruz, Institute for Particle Physics, Santa Cruz, California 95064, USA*
[18] *California Institute of Technology, Pasadena, California 91125, USA*
[19] *University of Cincinnati, Cincinnati, Ohio 45221, USA*
[20] *University of Colorado, Boulder, Colorado 80309, USA*
[21] *Colorado State University, Fort Collins, Colorado 80523, USA*
[22] *Universität Dortmund, Institut für Physik, D-44221 Dortmund, Germany*

[23] Technische Universität Dresden, Institut für Kern- und Teilchenphysik, D-01062 Dresden, Germany
[24] Laboratoire Leprince-Ringuet, CNRS/IN2P3, Ecole Polytechnique, F-91128 Palaiseau, France
[25] University of Edinburgh, Edinburgh EH9 3JZ, United Kingdom
[26] Università di Ferrara, Dipartimento di Fisica and INFN, I-44100 Ferrara, Italy
[27] Laboratori Nazionali di Frascati dell'INFN, I-00044 Frascati, Italy
[28] Università di Genova, Dipartimento di Fisica and INFN, I-16146 Genova, Italy
[29] Harvard University, Cambridge, Massachusetts 02138, USA
[30] Universität Heidelberg, Physikalisches Institut, Philosophenweg 12, D-69120 Heidelberg, Germany
[31] Imperial College London, London, SW7 2AZ, United Kingdom
[32] University of Iowa, Iowa City, Iowa 52242, USA
[33] Iowa State University, Ames, Iowa 50011-3160, USA
[34] Johns Hopkins University, Baltimore, Maryland 21218, USA
[35] Universität Karlsruhe, Institut für Experimentelle Kernphysik, D-76021 Karlsruhe, Germany
[36] Laboratoire de l'Accélérateur Linéaire, IN2P3/CNRS et Université Paris-Sud 11,
Centre Scientifique d'Orsay, B. P. 34, F-91898 ORSAY Cedex, France
[37] Lawrence Livermore National Laboratory, Livermore, California 94550, USA
[38] University of Liverpool, Liverpool L69 7ZE, United Kingdom
[39] Queen Mary, University of London, E1 4NS, United Kingdom
[40] University of London, Royal Holloway and Bedford New College, Egham, Surrey TW20 0EX, United Kingdom
[41] University of Louisville, Louisville, Kentucky 40292, USA
[42] University of Manchester, Manchester M13 9PL, United Kingdom
[43] University of Maryland, College Park, Maryland 20742, USA
[44] University of Massachusetts, Amherst, Massachusetts 01003, USA
[45] Massachusetts Institute of Technology, Laboratory for Nuclear Science, Cambridge, Massachusetts 02139, USA
[46] McGill University, Montréal, Québec, Canada H3A 2T8
[47] Università di Milano, Dipartimento di Fisica and INFN, I-20133 Milano, Italy
[48] University of Mississippi, University, Mississippi 38677, USA
[49] Université de Montréal, Physique des Particules, Montréal, Québec, Canada H3C 3J7
[50] Mount Holyoke College, South Hadley, Massachusetts 01075, USA
[51] Università di Napoli Federico II, Dipartimento di Scienze Fisiche and INFN, I-80126, Napoli, Italy
[52] NIKHEF, National Institute for Nuclear Physics and High Energy Physics, NL-1009 DB Amsterdam, The Netherlands
[53] University of Notre Dame, Notre Dame, Indiana 46556, USA
[54] Ohio State University, Columbus, Ohio 43210, USA
[55] University of Oregon, Eugene, Oregon 97403, USA
[56] Università di Padova, Dipartimento di Fisica and INFN, I-35131 Padova, Italy
[57] Laboratoire de Physique Nucléaire et de Hautes Energies,
IN2P3/CNRS, Université Pierre et Marie Curie-Paris6,
Université Denis Diderot-Paris7, F-75252 Paris, France
[58] University of Pennsylvania, Philadelphia, Pennsylvania 19104, USA
[59] Università di Perugia, Dipartimento di Fisica and INFN, I-06100 Perugia, Italy
[60] Università di Pisa, Dipartimento di Fisica, Scuola Normale Superiore and INFN, I-56127 Pisa, Italy
[61] Princeton University, Princeton, New Jersey 08544, USA
[62] Università di Roma La Sapienza, Dipartimento di Fisica and INFN, I-00185 Roma, Italy
[63] Universität Rostock, D-18051 Rostock, Germany
[64] Rutherford Appleton Laboratory, Chilton, Didcot, Oxon, OX11 0QX, United Kingdom
[65] DSM/Dapnia, CEA/Saclay, F-91191 Gif-sur-Yvette, France
[66] University of South Carolina, Columbia, South Carolina 29208, USA
[67] Stanford Linear Accelerator Center, Stanford, California 94309, USA
[68] Stanford University, Stanford, California 94305-4060, USA
[69] State University of New York, Albany, New York 12222, USA
[70] University of Tennessee, Knoxville, Tennessee 37996, USA
[71] University of Texas at Austin, Austin, Texas 78712, USA
[72] University of Texas at Dallas, Richardson, Texas 75083, USA
[73] Università di Torino, Dipartimento di Fisica Sperimentale and INFN, I-10125 Torino, Italy
[74] Università di Trieste, Dipartimento di Fisica and INFN, I-34127 Trieste, Italy
[75] IFIC, Universitat de Valencia-CSIC, E-46071 Valencia, Spain
[76] University of Victoria, Victoria, British Columbia, Canada V8W 3P6
[77] Department of Physics, University of Warwick, Coventry CV4 7AL, United Kingdom
[78] University of Wisconsin, Madison, Wisconsin 53706, USA
[79] Yale University, New Haven, Connecticut 06511, USA

(Dated: March 13, 2008)

We present a measurement of the branching fraction and photon energy spectrum for the decay $B \to X_s\gamma$ using data from the *BABAR* experiment. The data sample corresponds to an integrated

luminosity of 210 fb^{-1}, from which approximately 680 000 $B\overline{B}$ events are tagged by a fully reconstructed hadronic decay of one of the B mesons. In the decay of the second B meson, an isolated high–energy photon is identified. We measure $\mathcal{B}(B \to X_s\gamma) = (3.66 \pm 0.85_{\rm stat} \pm 0.60_{\rm syst}) \times 10^{-4}$ for photon energies E_γ above 1.9 GeV in the B rest frame. From the measured spectrum we calculate the first and second moments for different minimum photon energies, which are used to extract the heavy-quark parameters $m_{\rm b}$ and μ_π^2. In addition, measurements of the direct CP asymmetry and isospin asymmetry are presented.

PACS numbers: 13.20.He, 13.30.Ce, 12.39.Hg

INTRODUCTION

We present measurements of the branching fraction and photon energy spectrum of the rare radiative penguin decay $B \to X_s\gamma$ using $\Upsilon(4S) \to B\overline{B}$ events. We use a new technique where one of the B mesons (called the tag B) decays to hadrons and is fully reconstructed. This approach allows for the determination of the charge, flavor and momentum of both of the B mesons, and thus the photon spectrum can be determined in the rest frame of the signal B. The method results in an improved purity for the signal sample, allows separate measurements for charged and neutral B mesons and enables the measurement of the direct CP asymmetry A_{CP}. This approach is complementary to those used in previous studies [1, 2, 3, 4] and incurs different systematic uncertainties.

In the Standard Model (SM), the decay $b \to s\gamma$ proceeds via a flavor-changing neutral current. The decay is sensitive to new physics through non-SM heavy particles entering at the loop level [5]. Recent next-to-next-to-leading-order calculations predict SM branching fractions in the range $\mathcal{B}(B \to X_s\gamma) = (3.0 - 3.5) \times 10^{-4}$ for $E_\gamma > 1.6$ GeV with uncertainties that vary from 7% to 14% [6, 7, 8]. Here E_γ is the energy of the signal photon in the rest frame of the B meson, and the cutoff is chosen to avoid non-perturbative effects at lower energies. The current world average measured branching fraction is $\mathcal{B}(B \to X_s\gamma) = (3.55 \pm 0.26) \times 10^{-4}$ ($E_\gamma >$ 1.6 GeV) [9, 10]. The moments of the photon energy spectrum are sensitive to the Heavy Quark Expansion parameters m_b and μ_π^2, related to the mass and momentum of the b quark within the B meson [11]. Improved measurements of these parameters can be used to reduce the uncertainty in the CKM matrix elements $|V_{cb}|$ and $|V_{ub}|$ [9, 10].

The measurements presented here are based on a sample of 232 million $B\overline{B}$ pairs collected on the $\Upsilon(4S)$ resonance by the *BABAR* detector [12] at the PEP-II asymmetric-energy e^+e^- storage ring operating at SLAC, corresponding to an integrated luminosity of 210 fb^{-1}. After reconstruction of the tag B, the remaining particles in the event are assigned to the second B (the signal B) and events containing a high-energy photon are selected. The signal process $B \to X\gamma$ at this stage is taken to mean events from either $b \to s\gamma$ or $b \to d\gamma$ decays; the small contribution from $b \to d\gamma$ is subtracted at the end of the analysis. The sample also includes background from continuum (non-$B\overline{B}$) events and $B\overline{B}$ events in which the tag B is misreconstructed. These are subtracted by means of a fit to the beam-energy-subsituted mass (defined below) of the tag B.

The remaining background events, where the photon candidate is not from the signal process (e.g., a photon from a π^0 or η decay), are subtracted using a Monte Carlo (MC) model based on `EvtGen` [13] and `GEANT4` [14]. The MC predictions are scaled to data in the low E_γ region, where the signal contribution is very small. This allows a reliable measurement for photon energies $E_\gamma > 1.9$ GeV. Finally, to compare with other experiments and predictions, the measured rate is extrapolated using theoretical models to give the rate for $E_\gamma > 1.6$ GeV.

This measurement is currently limited by statistics, and furthermore, the dominant systematic errors are of the type that should decrease with a larger data sample. Therefore, the approach followed here is expected to provide an increasingly competitive level of precision when applied to the larger data sample currently being collected by the *BABAR* experiment.

EVENT SELECTION

Using 1114 exclusive hadronic decay channels [15], which represent about 5% of the total decay width of the B^0 and B^+ mesons, we identify events in which one of the two B mesons is fully reconstructed. The kinematic consistency of the tag B candidates is checked with two variables, the beam-energy-substituted mass $m_{\rm ES} = \sqrt{s/4 - \vec{p}_B^{\,2}}$, and the energy difference $\Delta E = E_B - \sqrt{s}/2$, where s is the total energy squared in the center-of-mass (c.m.) frame, and E_B and $\vec{p}_B$ are the the c.m. energy and momentum of the tag B candidate. We require $|\Delta E| \leq 60$ MeV, a window of approximately $\pm 3\sigma$.

Those particles in the event that are not reconstructed as part of the tag B are regarded as coming from the signal B. Among these particles we require an isolated photon candidate with energy $E_\gamma > 1.3$ GeV in the B frame. To ensure a well reconstructed photon, we require the electromagnetic shower to lie well within the calorimeter acceptance and to satisfy isolation and shower shape requirements.

The background events consist of non-signal B decays and continuum background from $u\overline{u}$, $d\overline{d}$, $s\overline{s}$ and $c\overline{c}$ events. The continuum events are suppressed by using a Fisher discriminant that combines 12 variables related to the different event decay topologies of $B\overline{B}$ and continuum events. These include event-shape variables such as the thrust, as well as information on the energy flow relative to the direction of the candidate signal photon.

To discriminate against photons from π^0 and η decays, we combine the signal candidate photon with any other photon in the event associated with the signal B. The event is vetoed if the pair's invariant mass is consistent with a π^0 or η. Furthermore, the event is rejected if the candidate photon combined with a $\pi^\pm$ is consistent with a $\rho^\pm \to \pi^\pm\pi^0$ decay assuming that the second photon from the π^0 decay is lost.

FIT OF SIGNAL RATES

The distribution of m_{ES} for the selected events has a peak around the mass of the B meson, corresponding to correctly reconstructed $B\overline{B}$ events, and a broad background component that stems from non-$B\overline{B}$ and misreconstructed $B\overline{B}$ events. The peak is modeled with a Crystal Ball (CB) function [16]. This contains two parameters that correspond to the mean and width of the Gaussian core and two additional parameters that describe a power-law tail extended to masses below the core region. The non-peak background term is described with an ARGUS function [17].

Applying the selection criteria outlined above yields approximately 7 700 events. We divide the event sample into 14 intervals of photon energy, each 100 MeV wide, spanning the range 1.3 to 2.7 GeV. In each interval, we extract the number of peak events with a binned maximum likelihood fit to the m_{ES} distribution.

The limited size of the data sample means that it is not possible to fit all of the parameters related to the shape of the CB and ARGUS functions individually in separate intervals of photon energy. One expects, however, a smooth variation of the shapes as a function of E_γ. To impose this smoothness, a simultaneous fit of the m_{ES} distributions for all of the photon-energy intervals is carried out. The variation of the shape parameters with photon energy is described by polynomials, whose orders are the lowest possible that allow an adequate modeling of the data. Examples of the m_{ES} distributions and results of the simultaneous fit are shown in Fig. 1. The global χ^2 is 330 for the charged B sample and 357 for the neutral sample, both for 387 degrees of freedom.

The measured numbers of B events are shown in Fig. 1 (c) as a function of photon energy. The points are from data; the solid histogram is from a $B\overline{B}$ MC sample that excludes the signal decay $B \to X\gamma$. Due to the large background at low energy the signal region is defined as $E_\gamma > 1.9$ GeV. This choice was optimized in MC studies. The MC prediction has been scaled by fitting to the data region between $1.3 < E_\gamma < 1.9$ GeV, taking into account the small contribution from $B \to X\gamma$ decays in that region. For $E_\gamma > 1.9$ GeV, we observe 119 ± 22 $B \to X\gamma$ signal events over a $B\overline{B}$ background of 145 ± 9 events.

For $1.3 < E_\gamma < 1.9$ GeV a comparison of the data and background gives a χ^2 of 9.7 for five degrees of freedom. The probability to observe a value at least this great is 8.4%. Our estimate of the systematic uncertainty in the background (described below) is in fact smaller than the observed data-background difference; therefore we regard this difference primarily as a statistical fluctuation.

To determine the partial branching fractions, we require the total number of $B\overline{B}$ events in the sample after selection of the tag B candidates. In a procedure analogous to that described for the m_{ES} fits in bins of E_γ, we divide the data into four intervals of estimated tag B candidate purity and perform a simultaneous fit of the m_{ES} distributions. We obtain approximately 680 000 $B\overline{B}$ events corresponding to an efficiency of 0.3%.

DETERMINING THE PHOTON SPECTRUM

The differential decay rate $(1/\Gamma_B)(d\Gamma/dE_\gamma)$ is measured in bins of the (B-frame) photon energy for $E_\gamma > 1.9$ GeV up to the kinematic limit at 2.6 GeV. It is estimated for the ith bin as

$$\frac{1}{\Gamma_B}\frac{d\Gamma_i}{dE_\gamma} = \frac{N_i - b_i}{\varepsilon_i N_B} , \qquad (1)$$

where N_i is the number of B events in the bin, b_i is the number of B mesons from decays other than $B \to X\gamma$, N_B is the total number of B mesons in the sample, and ε_i is the efficiency, which corrects for both acceptance and bin-to-bin resolution effects. The values b_i are determined by means of a simultaneous fit to the m_{ES} distributions as described previously, using a sample of MC data consisting of $B\overline{B}$ events excluding the signal decay $B \to X\gamma$. As the differential decay rate is normalized using the total width of the B meson, Γ_B, the integral of (1) over all photon energies yields the branching fraction. To evaluate the selection efficiency ε_i, we model the signal photon energy spectrum using the kinetic scheme [18] with $m_b = 4.60$ GeV and $\mu_\pi^2 = 0.4\,\mathrm{GeV}^2$. The value of ε_i is determined from

$$\varepsilon_i = \frac{N_{\mathrm{found},i}/N_{\mathrm{sim}}}{N_{\mathrm{true},i}/N_{\mathrm{gen}}}\, C_{\mathrm{tag}} , \qquad (2)$$

where $N_{\mathrm{found},i}$ is the number of events found in a MC sample of $B \to X_s\gamma$ with detector simulation and N_{sim} is the number of events in the simulated sample. These

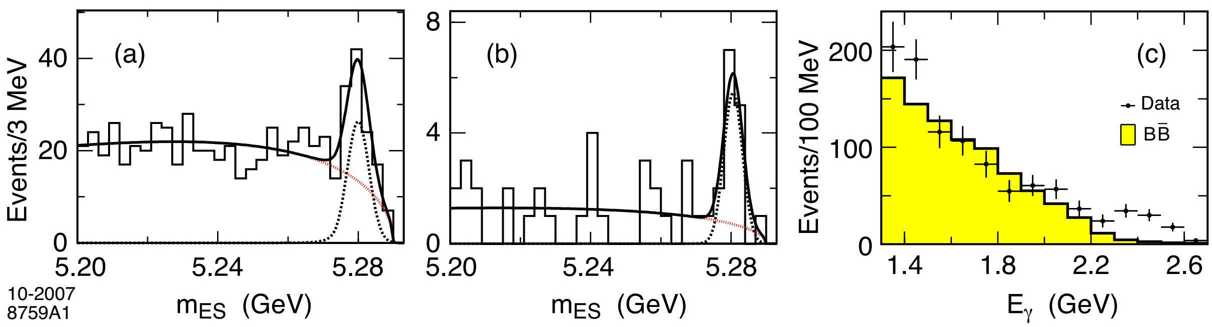

FIG. 1: Fits to the distribution of the beam-energy-substituted mass $m_{\rm ES}$ for two E_γ regions. The dashed curve shows the CB term and the dotted curve is the ARGUS term, corresponding to B and non-B events, respectively; the solid curve is their sum. (a) $1.6\,\text{GeV} < E_\gamma < 1.7\,\text{GeV}$ for the charged B sample. (b) $2.3\,\text{GeV} < E_\gamma < 2.4\,\text{GeV}$ for the neutral B sample. (c) The measured numbers of B events as a function of photon energy. The points are from data; the histogram is from a $B\overline{B}$ MC sample which excludes the signal decay $B \to X\gamma$.

quantities are found using the same fit procedure as applied to the real data for N_i and N_B. In the denominator of (2), $N_{\text{true},i}$ is the true number of events with photon energies in bin i and N_{gen} is the total number of events generated. These values are determined using the event generator for $B \to X_s\gamma$ decays only, without detector simulation. The factor C_{tag}, estimated using the MC model, corrects for the small dependence of the probability to find a tag B on the presence of a $B \to X\gamma$ final state. The efficiency increases roughly linearly with photon energy, and is approximately 30% (65%) for $E_\gamma = 1.9\,\text{GeV}$ (2.6 GeV).

To compare with other results we subtract the $B \to X_d\gamma$ component from the differential decay rates using the Standard Model prediction (for the CP and isospin asymmetries discussed below, however, we do not make this correction). The values $\mathcal{B}(B \to X_d\gamma)$ and $\mathcal{B}(B \to X_s\gamma)$ are in the ratio $|V_{td}/V_{ts}|^2$ assuming the same efficiency for the two categories of events. Therefore, the branching ratio is lowered by $(4.0 \pm 0.4)\%$ [19, 20].

SYSTEMATIC UNCERTAINTIES

There are four main sources of systematic uncertainty, which are summarized in Table I: modeling of the $B\overline{B}$ background, the $m_{\rm ES}$ fits, detector response and dependence on the $B \to X_s\gamma$ signal model. In addition there is an uncertainty from the subtraction of the $B \to X_d\gamma$ contribution.

After subtraction of the non-peak background using the $m_{\rm ES}$ distribution, the remaining background is mainly composed of $B\overline{B}$ events with the selected photon coming from a π^0 or η decay. Photons from π^0 account for 55% to 65% depending on E_γ and the charge of the tag B, while the contribution from η mesons varies from 18% to 29%. The remaining backgrounds include fake photons from $\bar{n}$ annihilation, real photons from bremsstrahlung or from ω decays, and electromagnetic showers from $e^\pm$ misidentified as photons. As the MC prediction for the $B\overline{B}$ background is scaled to the data at low energy, there is no uncertainty stemming from the absolute rate, but rather only from the shape of the distribution as a function of E_γ. The uncertainty from the inclusive π^0 and η spectra is investigated by using E_γ dependent correction factors for the π^0 and η yields from a large control sample of $B \to X\gamma$ candidate events, obtained using a lepton tag. These correction factors are typically around 5% for π^0 yields while they can be up to 30% for η yields. The remaining backgrounds have a roughly linear slope with E_γ; this is varied by $\pm 30\%$. We use the difference obtained with the modified MC compared to the standard MC simulation as a systematic uncertainty.

To assess the uncertainty related to the parameterization chosen for the $m_{\rm ES}$ fit, additional coefficients are introduced that allow linear or higher-order dependence of the CB and ARGUS function shape parameters on the photon energy. The maximum variation in the fitted rates is taken as the systematic uncertainty. A similar set of variations for the dependence of the shape parameters on the B meson purity is carried out for the $m_{\rm ES}$ fits used to determine the total number of B mesons in the data sample. To allow for a small peaking component in the distribution of $m_{\rm ES}$ from $B^\pm$ decays reconstructed as B^0 ($\overline{B}^0$) decays and vice versa, we remove these events from the MC sample and take the difference in the result as a systematic uncertainty.

The uncertainties related to the detector modeling and event reconstruction are estimated by comparing MC simulations of track and photon efficiencies as well as particle identification efficiencies with data control samples. From these comparisons we estimate corresponding systematic errors, which are in all cases small compared to other uncertainties.

To assess the uncertainty in the efficiency due to the assumed shape of the E_γ spectrum, we vary m_b and μ_π^2

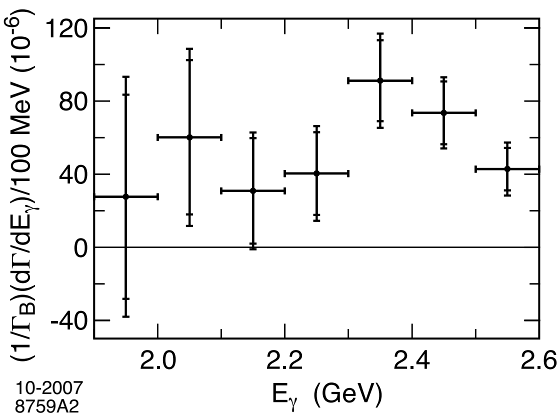

FIG. 2: The partial branching fractions $(1/\Gamma_B)(d\Gamma/dE_\gamma)$ with statistical (inner) and total (outer) uncertainties.

in the kinetic scheme by $\pm 0.1\,\mathrm{GeV}$ and $\pm 0.1\,\mathrm{GeV}^2$, respectively. These variations are large compared to the uncertainties in the world average [10] in order to cover alternative Ansätze for the the heavy quark distribution function [21, 22]. They also account for uncertainties related to the small rate of $B \to X\gamma$ decays expected below 1.9 GeV.

TABLE I: Results for the differential decay rate $(1/\Gamma_B)(d\Gamma/dE_\gamma)$ and moments of the photon spectrum with statistical and systematic errors. The major contributions to the systematic uncertainties are also listed: (a) background modeling, (b) m_{ES} fit parameterization, (c) detector response, (d) $B \to X_s\gamma$ model.

$(1/\Gamma_B)(d\Gamma/dE_\gamma)\,(10^{-4})$							
E_γ (GeV)	Value	σ_{stat}	σ_{syst}	(a)	(b)	(c)	(d)
1.9-2.0	0.28	0.56	0.34	0.26	0.13	0.19	0.03
2.0-2.1	0.60	0.42	0.24	0.18	0.12	0.08	0.05
2.1-2.2	0.31	0.29	0.14	0.11	0.06	0.03	0.03
2.2-2.3	0.40	0.23	0.13	0.07	0.05	0.09	0.03
2.3-2.4	0.91	0.22	0.13	0.07	0.08	0.05	0.06
2.4-2.5	0.74	0.17	0.09	0.05	0.05	0.02	0.05
2.5-2.6	0.43	0.12	0.09	0.03	0.03	0.07	0.04
$\langle E_\gamma \rangle$ (GeV)							
E_γ (GeV)	Value	σ_{stat}	σ_{syst}	(a)	(b)	(c)	(d)
1.9-2.6	2.289	0.058	0.027	0.018	0.019	0.009	0.002
2.0-2.6	2.315	0.036	0.019	0.013	0.011	0.009	0.001
2.1-2.6	2.371	0.025	0.009	0.007	0.005	0.003	0.001
2.2-2.6	2.398	0.016	0.004	0.003	0.003	0.001	0.000
2.3-2.6	2.427	0.010	0.006	0.000	0.001	0.005	0.000
$\langle (E_\gamma - \langle E_\gamma \rangle)^2 \rangle$ (GeV^2)							
E_γ (GeV)	Value	σ_{stat}	σ_{syst}	(a)	(b)	(c)	(d)
1.9-2.6	0.0334	0.0124	0.0062	0.0040	0.0025	0.0037	0.0013
2.0-2.6	0.0265	0.0057	0.0024	0.0018	0.0010	0.0007	0.0011
2.1-2.6	0.0142	0.0037	0.0013	0.0009	0.0005	0.0004	0.0006
2.2-2.6	0.0092	0.0015	0.0010	0.0002	0.0002	0.0009	0.0003
2.3-2.6	0.0059	0.0007	0.0003	0.0000	0.0000	0.0003	0.0002

RESULTS

The partial branching fractions $(1/\Gamma_B)(d\Gamma/dE_\gamma)$ are shown in Fig. 2 after all corrections. The inner error bars show the statistical uncertainties. The outer error bars show the quadratic sum of the statistical and systematic terms. By integrating the spectrum, we obtain $\mathcal{B}(B \to X_s\gamma) = (3.66 \pm 0.85_{\mathrm{stat}} \pm 0.60_{\mathrm{syst}}) \times 10^{-4}$. The results for the differential decay rate and for the moments of the photon energy spectrum for various minimum photon energies E_{cut} are given in Table I. The branching fraction for larger values of E_{cut} and the correlations between the measurements are given in Tables II-V. Our results are in good agreement with those presented in Refs. [1, 2, 3, 4].

We also measure the isospin asymmetry Δ_{0-},

$$\Delta_{0-} = \frac{\Gamma(\overline{B}^0 \to X_{s,d}\,\gamma) - \Gamma(B^- \to X_{s,d}\,\gamma)}{\Gamma(\overline{B}^0 \to X_{s,d}\,\gamma) + \Gamma(B^- \to X_{s,d}\,\gamma)}\,, \quad (3)$$

where inclusion of charge conjugate modes is implied. It has been argued that enhanced power corrections to the $B \to X_s\gamma$ rate could also lead to values of Δ_{0-} as large as $+10\%$ [23]. Therefore, experimental measurements of Δ_{0-} can help determine the size of these effects and hence reduce the theoretical uncertainty on the total rate. To obtain decay rates from the branching fractions we use the B meson lifetimes: $\tau(B^0) = 1.530 \pm 0.008$ ps and $\tau(B^+) = 1.638 \pm 0.011$ ps [24]. For photon energies greater than 2.2 GeV, we obtain $\Delta_{0-} = -0.06 \pm 0.15_{\mathrm{stat}} \pm 0.07_{\mathrm{syst}}$.

The direct CP asymmetry A_{CP},

$$A_{CP} = \frac{\mathcal{B}(B \to X_{s,d}\,\gamma) - \mathcal{B}(\overline{B} \to X_{s,d}\,\gamma)}{\mathcal{B}(B \to X_{s,d}\,\gamma) + \mathcal{B}(\overline{B} \to X_{s,d}\,\gamma)} \frac{1}{1-2\omega}\,, \quad (4)$$

is measured by splitting the tag sample into B and $\overline{B}$ mesons. The dilution factor $\frac{1}{1-2\omega}$ accounts for the mistag fraction ω, here simply the time integrated B^0 mixing probability of $\chi_d = 0.188 \pm 0.003$ [24] multiplied by the fraction of B^0 events in the total data sample. A_{CP} can be significantly enhanced by new physics [19] while in the SM it is predicted to be around 10^{-9} [25, 26]. We obtain a value of $A_{CP} = 0.10 \pm 0.18_{\mathrm{stat}} \pm 0.05_{\mathrm{syst}}$ for photon energies above 2.2 GeV.

For both Δ_{0-} and A_{CP}, a photon energy cutoff of 2.2 GeV is chosen because it facilitates comparison with previous results and minimizes the total uncertainty. Our results are in good agreement with previous measurements [3, 4, 27, 28, 29].

Finally, we use heavy quark expansions in the kinetic scheme [18] and our measurements of the E_γ moments to determine the parameters m_b and μ_π^2. We include the theoretical uncertainties quoted in Ref. [18] in the overall covariance matrix used in the fit. To minimize

the theoretical uncertainty we only use moments with $E_{\rm cut} \leq 2.0\,{\rm GeV}$ and obtain $m_b = 4.46^{+0.21}_{-0.23}\,{\rm GeV}$ and $\mu_\pi^2 = 0.64^{+0.39}_{-0.38}\,{\rm GeV}^2$ with a correlation of $\rho = -0.94$.

CONCLUSIONS

We have measured the $B \to X_s\gamma$ branching fraction and moments of the photon energy spectrum above several minimum photon energies. We find $\mathcal{B}(B \to X_s\gamma) = (3.66 \pm 0.85_{\rm stat} \pm 0.60_{\rm syst}) \times 10^{-4}$ for photon energies E_γ above 1.9 GeV. Dividing by an extrapolation factor of 0.936 ± 0.010 [10] we obtain $\mathcal{B}(B \to X_s\gamma) = (3.91 \pm 0.91_{\rm stat} \pm 0.64_{\rm syst}) \times 10^{-4}$ for $E_\gamma > 1.6\,{\rm GeV}$. The moments of the spectrum can be used to improve the knowledge of the heavy quark parameters m_b and μ_π^2; we obtain $m_b = 4.46^{+0.21}_{-0.23}\,{\rm GeV}$ and $\mu_\pi^2 = 0.64^{+0.39}_{-0.38}\,{\rm GeV}^2$ in the kinetic scheme. In addition we measured the isospin asymmetry $\Delta_{0-} = -0.06 \pm 0.15_{\rm stat} \pm 0.07_{\rm syst}$ and direct *CP* asymmetry $A_{CP} = 0.10 \pm 0.18_{\rm stat} \pm 0.05_{\rm syst}$ for photon energies above 2.2 GeV. The full reconstruction (recoil) method provides an almost background free measurement above photon energies of 2.2 GeV. Although statistics are limited at present, this approach is expected to provide a competitive measurement of the decay $B \to X_s\gamma$ with the larger data sample that is being accumulated at the B -Factories, in particular as the main systematic uncertainties will also be reduced with a larger data sample.

We are grateful for the excellent luminosity and machine conditions provided by our PEP-II colleagues, and for the substantial dedicated effort from the computing organizations that support *BABAR*. The collaborating institutions wish to thank SLAC for its support and kind hospitality. This work is supported by DOE and NSF (USA), NSERC (Canada), CEA and CNRS-IN2P3 (France), BMBF and DFG (Germany), INFN (Italy), FOM (The Netherlands), NFR (Norway), MES (Russia), MEC (Spain), and STFC (United Kingdom). Individuals have received support from the Marie Curie EIF (European Union) and the A. P. Sloan Foundation.

---

* Deceased
† Now at Temple University, Philadelphia, Pennsylvania 19122, USA
‡ Now at Tel Aviv University, Tel Aviv, 69978, Israel
§ Also with Università di Perugia, Dipartimento di Fisica, Perugia, Italy
¶ Also with Università della Basilicata, Potenza, Italy
** Also with Università di Sassari, Sassari, Italy

[1] CLEO Collaboration, S. Chen *et al.*, Phys. Rev. Lett. **87**, 251807 (2001).
[2] Belle Collaboration, P. Koppenburg *et al.*, Phys. Rev. Lett. **93**, 061803 (2004).
[3] *BABAR* Collaboration, B. Aubert *et al.*, Phys. Rev. **D72**, 052004 (2005).
[4] *BABAR* Collaboration, B. Aubert *et al.*, Phys. Rev. Lett. **97**, 171803 (2006).
[5] T. Hurth, Rev. Mod. Phys. **75**, 1159 (2003), and references therein.
[6] M. Misiak *et al.*, Phys. Rev. Lett. **98**, 022002 (2007).
[7] T. Becher and M. Neubert, Phys. Lett. **B637**, 251 (2006).
[8] J. R. Andersen and E. Gardi, JHEP **01**, 029 (2007).
[9] Heavy Flavor Averaging Group (HFAG), E. Barberio *et al.*, (2007), arXiv:0704.3575.
[10] O. Buchmueller and H. Flaecher, Phys. Rev. **D73**, 073008 (2006).
[11] A. Kapustin and Z. Ligeti, Phys. Lett. **B355**, 318 (1995).
[12] *BABAR* Collaboration, B. Aubert *et al.*, Nucl. Instrum. Meth. **A479**, 1 (2002).
[13] D. J. Lange, Nucl. Instrum. Meth. **A462**, 152 (2001).
[14] GEANT4 Collaboration, S. Agostinelli *et al.*, Nucl. Instrum. Meth. **A506**, 250 (2003).
[15] *BABAR* Collaboration, B. Aubert *et al.*, Phys. Rev. Lett. **92**, 071802 (2004).
[16] M.J. Oreglia, Ph.D. Thesis, SLAC-236 (1980), App. D; J.E. Gaiser, Ph.D. Thesis, SLAC-255 (1982), App. F; T. Skwarnicki, Ph.D. Thesis, DESY F31-86-02 (1986), App. E.
[17] ARGUS Collaboration, H. Albrecht *et al.*, Phys. Lett. **B185**, 218 (1987).
[18] D. Benson, I. I. Bigi, and N. Uraltsev, Nucl. Phys. **B710**, 371 (2005).
[19] T. Hurth, E. Lunghi, and W. Porod, Nucl. Phys. **B704**, 56 (2005).
[20] CKMfitter Group, J. Charles *et al.*, Eur. Phys. J. **C41**, 1 (2005).
[21] A. L. Kagan and M. Neubert, Eur. Phys. J. **C7**, 5 (1999).
[22] B. O. Lange, M. Neubert, and G. Paz, Phys. Rev. **D72**, 073006 (2005).
[23] S. J. Lee, M. Neubert, and G. Paz, Phys. Rev. **D75**, 114005 (2007).
[24] Particle Data Group, W. M. Yao *et al.*, J. Phys. **G33**, 1 (2006).
[25] J. M. Soares, Nucl. Phys. **B367**, 575 (1991).
[26] T. Hurth and T. Mannel, Phys. Lett. **B511**, 196 (2001).
[27] CLEO Collaboration, T. E. Coan *et al.*, Phys. Rev. Lett. **86**, 5661 (2001).
[28] *BABAR* Collaboration, B. Aubert *et al.*, Phys. Rev. Lett. **93**, 021804 (2004).
[29] Belle Collaboration, S. Nishida *et al.*, Phys. Rev. Lett. **93**, 031803 (2004).

TABLE II: Results for $\mathcal{B}(B \to X_s\gamma)$ for different minimum photon energies with statistical and systematic errors. Details on the major contributions to the systematic uncertainties are also given.

				$\mathcal{B}(B \to X_s\gamma)$ (10^{-4})			
E_γ range (GeV)	Value	$\sigma_{\rm stat}$	$\sigma_{\rm syst}$	Background modeling	$m_{\rm ES}$ fit parameterization	Detector response	$B \to X_s\gamma$ model
1.9-2.6	3.66	0.85	0.60	0.35	0.45	0.18	0.08
2.0-2.6	3.39	0.64	0.47	0.31	0.34	0.07	0.06
2.1-2.6	2.78	0.48	0.35	0.22	0.24	0.08	0.05
2.2-2.6	2.48	0.38	0.27	0.14	0.19	0.10	0.05
2.3-2.6	2.07	0.30	0.20	0.10	0.15	0.04	0.05

TABLE III: Correlations between the systematic uncertainties for the differential decay rate measurements. (The statistical correlations between E_γ bins are negligible.)

E_γ interval	$(1/\Gamma_B)(d\Gamma/dE_\gamma)$						
(GeV)	1.9-2.0	2.0-2.1	2.1-2.2	2.2-2.3	2.3-2.4	2.4-2.5	2.5-2.6
1.9-2.0	1.000	-0.004	0.311	0.949	-0.108	0.083	0.849
2.0-2.1		1.000	0.912	0.096	0.805	0.721	-0.087
2.1-2.2			1.000	0.352	0.712	0.699	0.152
2.2-2.3				1.000	0.111	0.310	0.940
2.3-2.4					1.000	0.969	0.115
2.4-2.5						1.000	0.341
2.5-2.6							1.000

TABLE IV: Statistical correlations between $\langle E_\gamma\rangle$ and $\langle(E_\gamma - \langle E_\gamma\rangle)^2\rangle$ measurements with different minimum photon energies E_γ.

E_γ range		$\langle E_\gamma\rangle$					$\langle(E_\gamma - \langle E_\gamma\rangle)^2\rangle$				
(GeV)		1.9-2.6	2.0-2.6	2.1-2.6	2.2-2.6	2.3-2.6	1.9-2.6	2.0-2.6	2.1-2.6	2.2-2.6	2.3-2.6
	1.9-2.6	1.000	0.503	0.195	0.053	-0.001	-0.897	-0.419	-0.180	-0.040	0.041
	2.0-2.6		1.000	0.418	0.141	0.027	-0.310	-0.807	-0.368	-0.093	0.069
$\langle E_\gamma\rangle$	2.1-2.6			1.000	0.427	0.157	-0.124	-0.342	-0.822	-0.244	0.109
	2.2-2.6				1.000	0.408	-0.017	-0.054	-0.153	-0.550	0.200
	2.3-2.6					1.000	0.008	0.019	0.032	0.095	0.363
	1.9-2.6						1.000	0.266	-0.041	-0.048	0.054
	2.0-2.6							1.000	0.094	-0.052	0.113
$\langle(E_\gamma - \langle E_\gamma\rangle)^2\rangle$	2.1-2.6								1.000	0.177	0.144
	2.2-2.6									1.000	0.350
	2.3-2.6										1.000

TABLE V: Systematic correlations between $\langle E_\gamma\rangle$ and $\langle(E_\gamma - \langle E_\gamma\rangle)^2\rangle$ measurements with different minimum photon energies E_γ.

E_γ range		$\langle E_\gamma\rangle$					$\langle(E_\gamma - \langle E_\gamma\rangle)^2\rangle$				
(GeV)		1.9-2.6	2.0-2.6	2.1-2.6	2.2-2.6	2.3-2.6	1.9-2.6	2.0-2.6	2.1-2.6	2.2-2.6	2.3-2.6
	1.9-2.6	1.000	0.556	0.811	0.707	0.128	0.298	0.875	0.599	-0.030	-0.013
	2.0-2.6		1.000	0.946	0.667	0.751	0.903	0.511	0.943	0.775	0.724
$\langle E_\gamma\rangle$	2.1-2.6			1.000	0.765	0.653	0.741	0.771	0.932	0.553	0.546
	2.2-2.6				1.000	0.527	0.412	0.777	0.731	0.307	0.416
	2.3-2.6					1.000	0.745	0.102	0.658	0.911	0.964
	1.9-2.6						1.000	0.253	0.841	0.868	0.770
	2.0-2.6							1.000	0.656	-0.059	-0.019
$\langle(E_\gamma - \langle E_\gamma\rangle)^2\rangle$	2.1-2.6								1.000	0.627	0.597
	2.2-2.6									1.000	0.967
	2.3-2.6										1.000